

# A Three-Dimensional Carbon Nanotube/Graphene Sandwich and Its Application as Electrode in Supercapacitors

By Zhuangjun Fan,\* Jun Yan, Linjie Zhi,\* Qiang Zhang, Tong Wei, Jing Feng, Milin Zhang, Weizhong Qian, and Fei Wei\*

Owing to its unique electrical, thermal, and mechanical properties, graphene has attracted great attention in various application areas, such as energy-storage materials,<sup>[1–3]</sup> free-standing paper-like materials,<sup>[4–6]</sup> polymer composites,<sup>[7–9]</sup> liquid crystal devices,<sup>[10]</sup> and mechanical resonators.<sup>[11,12]</sup> Approaches for preparing graphene include micromechanical cleavage,<sup>[11,13,14]</sup> chemical vapor deposition (CVD),<sup>[15]</sup> solvent thermal reaction,<sup>[16,17]</sup> thermal desorption of Si from SiC substrates,<sup>[18]</sup> and chemical routes via carbon nanotubes (CNTs), graphite intercalation compounds (GIC) or graphite oxide (GO).<sup>[19–22]</sup> Among these, the oxidation and reduction of graphite is one of the most effective methods in mass production of graphene for industrial applications.<sup>[12,23]</sup> However, the reduction of GO results in always a gradual decrease of its hydrophilic character, which leads to irreversible agglomeration and precipitation;<sup>[24,25]</sup> though GO itself is highly hydrophilic and can form stable dispersion in aqueous solvents.<sup>[26]</sup> As a result, the unique 2D feature of graphene would be lost. Chemical functionalization or electrostatic stabilization have been reported to be useful to suppress the aggregation of graphene,<sup>[27]</sup> but the pristine properties of graphene would be therefore hindered some how.<sup>[2,28]</sup>

Attempts to combine CNTs and graphene have been made to prepare transparent conductors<sup>[26]</sup> and electrode materials for rechargeable lithium ion secondary batteries.<sup>[29]</sup> Significant property enhancement has been observed in these materials with the existence of CNTs which are believed to bridge the defects for electron transfer and, in the mean time, to increase the basal

spacing between graphene sheets. Recently, a novel 3D carbon material, consisting of parallel graphene layers stabilized by vertically aligned CNTs in between the graphene planes, has been designed by computational model.<sup>[29]</sup> Monte Carlo simulations revealed that this novel material doped with lithium cations can reach hydrogen storage capacity of 41 g L<sup>-1</sup>, which would meet the D.O.E's volumetric target for mobile applications under ambient conditions. However, experimental fabrication of this material is challengeable. In this communication, for the first time, we report a novel strategy to prepare 3D CNT/graphene sandwich (CGS) structures with CNT pillars grown in between the graphene layers by CVD approach (**Scheme 1**). The CGS has been used successfully as electrodes in supercapacitors, and a maximum specific capacitance of 385 F g<sup>-1</sup> has been obtained at a scan rate of 10 mV s<sup>-1</sup> in 6 M KOH aqueous solution.

Although the growth of aligned CNTs in between the vermiculite layers has been achieved successfully recently,<sup>[30]</sup> experimental investigation demonstrated that most of the CNTs grown on graphite substrate is not uniform due to the poor wettability between graphite surface and catalyst particles, which results in aggregation and then coalescence of the catalyst particles on the graphite substrate during sintering.<sup>[31]</sup> Therefore, exfoliated graphene oxide (~1 nm in thickness, Figure S1, see Supporting Information) is selected here as the substrate to grow CNTs due to its high surface energy (62.1 mJ m<sup>-2</sup>) as compared to graphene (46.7 mJ m<sup>-2</sup>) and graphite (54.8 mJ m<sup>-2</sup>),<sup>[32]</sup> and its feasibility of being reduced into graphene.

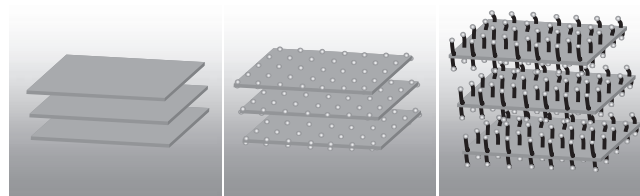
Scanning electron microscopy (SEM) characterization of a typical CGS sample disclosed that graphene-CNT-graphene sandwich structure has been obtained (**Figure 1a**). CNTs are grown in between the graphene sheets and distributed uniformly but sparsely on the whole sheet surface. Indeed, Brunauer–Emmett–Teller (BET) surface area of CGS

[\*] Prof. Z. J. Fan, Dr. J. Yan, Prof. T. Wei, Prof. J. Feng, Prof. M. L. Zhang  
Key Laboratory of Superlight Materials and Surface Technology  
Ministry of Education  
College of Material Science and Chemical Engineering  
Harbin Engineering University  
Harbin 150001 (P. R. China)  
E-mail: fanzhj666@163.com

Prof. L. J. Zhi  
National Center for Nanoscience and Technology of China  
Zhongguancun, Beiyitiao 11  
Beijing 100190 (P. R. China)  
E-mail: zhilj@nanoctr.cn

Prof. F. Wei, Prof. W. Z. Qian, Dr. Q. Zhang  
Beijing Key Laboratory of Green Chemical Reaction Engineering  
and Technology  
Department of Chemical Engineering, Tsinghua University  
Beijing 100084 (P. R. China)  
E-mail: weifei@flotu.org

DOI: 10.1002/adma.201001029



**Scheme 1.** Illustration of the formation of hybrid materials with CNTs grown in between graphene nanosheets, showing stacked layers of graphene oxide (left), catalyst particles adhered onto layer surface after deposition (middle), and CNTs in between graphene layers after growth (right).

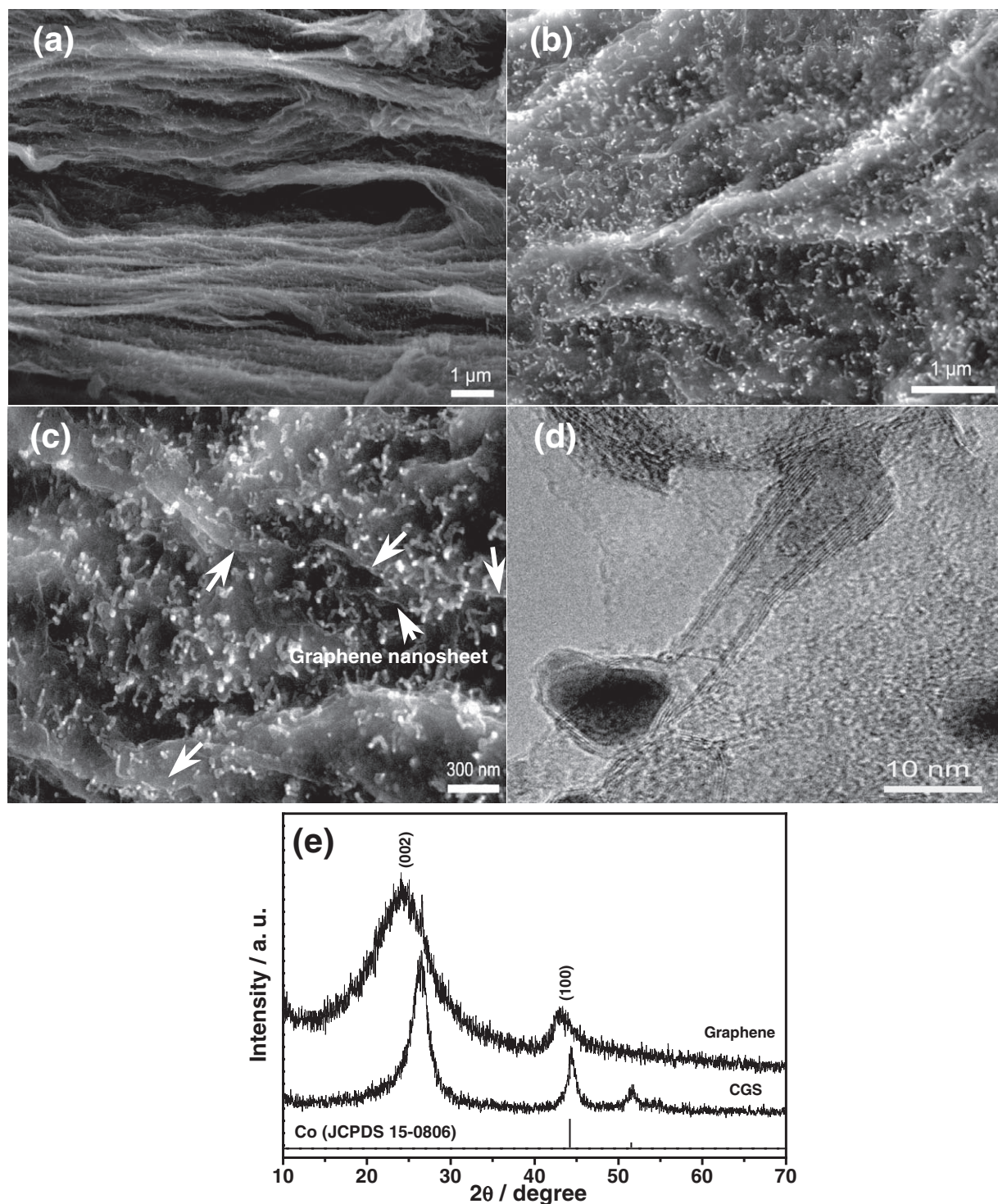


**Figure 1.** a–c) SEM images and d) TEM image of CGS (Co catalyst: 16 wt%; carbon source: CO). e) XRD patterns of graphene nanosheets and CGS.

( $612 \text{ m}^2 \text{ g}^{-1}$ ) is much higher than that of graphene ( $202 \text{ m}^2 \text{ g}^{-1}$ ), and this surface area improvement should be mainly due to the effective intercalation and distribution of CNTs in between the graphenes. In addition, the enlarged view of the hybrid material reveals that the distance between CNTs is about

100–200 nm, and the majority of the CNTs is less than 100 nm in length (Figure 1b and c). Transmission electron microscope (TEM) observation shows that the obtained CNTs are mainly multi-walled CNTs with an inner diameter of 5–7 nm, and an outer diameter of about 7–12 nm (Figure 1d). Most of

the cobalt based catalysts reside at the top of the CNTs, suggesting the tip growth mechanism due to the poor binding strength between the catalytic particle and the catalyst support.<sup>[33]</sup> Energy dispersive X-ray spectra (EDX, Figure S2, see Supporting Information) showed that the chemical composition of C:Co:O is 83:16:1 (weight ratio) after CNT growth, suggesting that the catalyst particles are mainly cobalt, which was further confirmed by X-ray diffraction analysis (XRD, Figure 1e). Raman characterization (Figure S3, see Supporting Information) demonstrated that the intensity ratio ( $I_D/I_G$ ) of D band and G band of GO is about 0.96, whereas the  $I_D/I_G$  of CGS is 0.72, implying that the graphitic crystalline structure of the CGS is much better than that of GO. Furthermore, we pressed graphene based materials into a disc of 15 mm diameter in order to measure the conductivity. The vertical and parallel conductivities of CGS are 40.7 and 180.1 S m<sup>-1</sup>, respectively, while 6.2 and 120.5 S m<sup>-1</sup> are obtained for pure graphene material. It means that the incorporation of CNTs in between the graphene sheets can improve the electrical connectivity between the sheets and CNTs.

Notably, the catalyst concentration and carbon source significantly affect the morphologies of obtained CNTs. It was observed that carbon monoxide as a carbon source for growing CNTs had

a tendency of forming aligned, sparse and short CNTs.<sup>[34]</sup> While methane as carbon source, low catalyst concentration (Co: 20 wt%) tend to produce long CNTs (1–2 μm) with a compact layer randomly covering on the surface of graphene (Figure 2a and b). Furthermore, high catalyst concentration (Co: 60 wt%) led to sometimes aggregation of catalyst particles and encapsulation with graphene layers (Figure 2c and d) during heat treatment, and thus losing their catalytic activity for nanotube growth. This is consistent with the results proposed by Liao et al.<sup>[35]</sup>

Based on the unique carbonaceous sandwich structures, the 3D CGS would be expected to hold good electron conductivity, low diffusion resistance to protons/cations, easy electrolyte penetration, and high electroactive areas to be a promising candidate for the fabrication of high performance supercapacitors. Recently, graphene has been used as electrodes for supercapacitors, and specific capacitance of 135 F g<sup>-1</sup> in aqueous KOH and 117 F g<sup>-1</sup> in H<sub>2</sub>SO<sub>4</sub> electrolyte have been obtained based on double layer capacitance from the interconnected open channels between graphene layers distributed in a 2D architecture.<sup>[36,37]</sup> In view of the combination of both double-layer capacitance from graphene and pseudo-capacitance from catalyst, CGS as electrode would be expected to have better electrochemical performance.

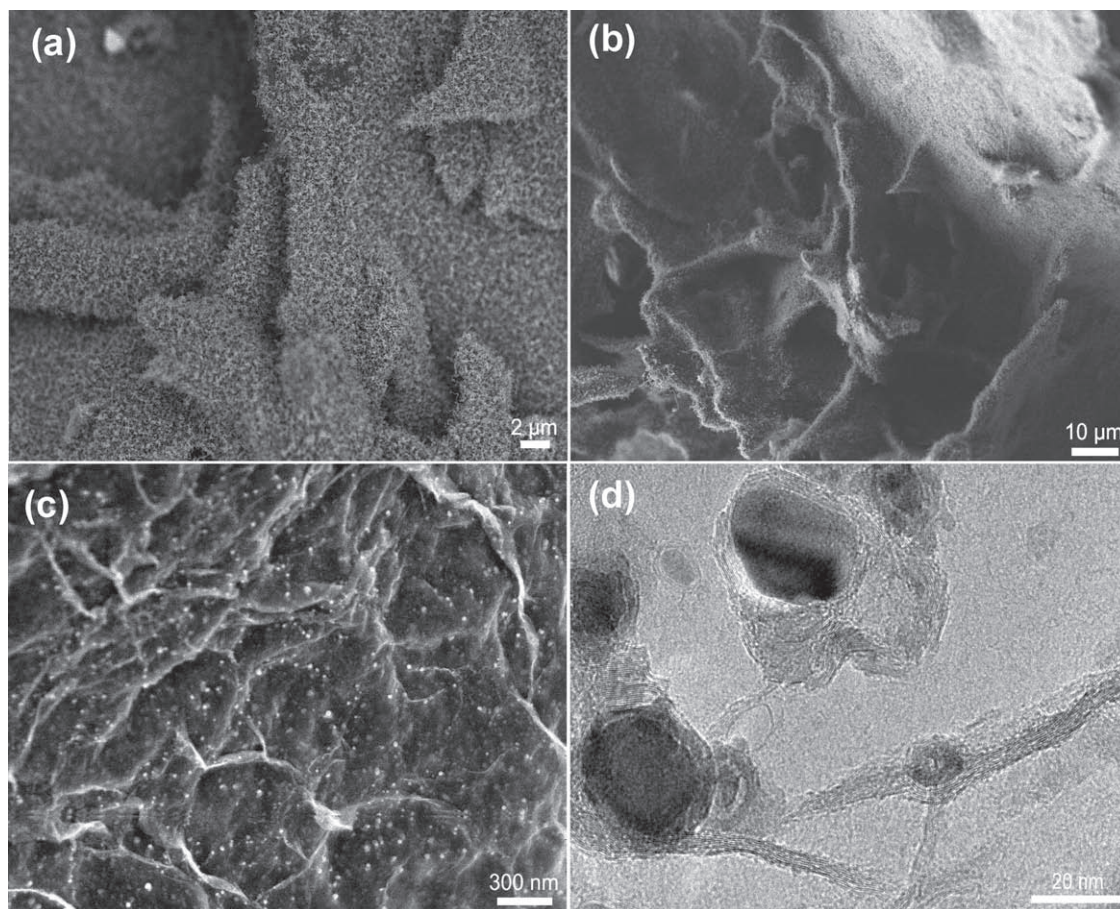


**Figure 2.** a,b) SEM images of the hybrid material with CNTs covering on the surfaces of graphene (Co catalyst: 16 wt%; carbon source: C<sub>2</sub>H<sub>4</sub>). c) SEM and d) TEM images of carbon/cobalt core/shell structures on the graphene sheets (Co catalyst: 60 wt%; carbon source: CO).

In the potential range from  $-1.0$  to  $-0.2$  V, it can be seen that the anodic peak current occurs at about  $-0.62$  V in the previous two cycles of cyclic voltammetry (CV) curves for CGS (carbon source: carbon monoxide; Co: 16 wt%) at a scan rate of  $10 \text{ mV s}^{-1}$  (Figure S4, see the Supporting Information), which corresponds to the conversion reaction of cobalt particles in alkaline solution ( $\text{Co} + 2\text{OH}^- = \text{Co}(\text{OH})_2 + 2 \text{e}^-$ ).<sup>[38]</sup> This reaction is irreversible because its cathodic peak is negligible compared with the anodic. In the following cycles, CV curves exhibit a fairly rectangular shape which is typical for double layer capacitors. As for CV curves measured in the potential window from  $-0.2$  to  $0.45$  V, strong redox peaks are visible as shown in Figure 3a, suggesting the high pseudocapacitance of cobalt hydroxide. The obvious increase of current along with scan rates suggests a good rate capability for this hybrid composite electrode. Furthermore, the discharge curves of CGS at different current densities (Figure S5, see Supporting Information) exhibit that the discharge time from  $0.4$  to  $0.15$  V is about two times longer than that from  $-0.2$

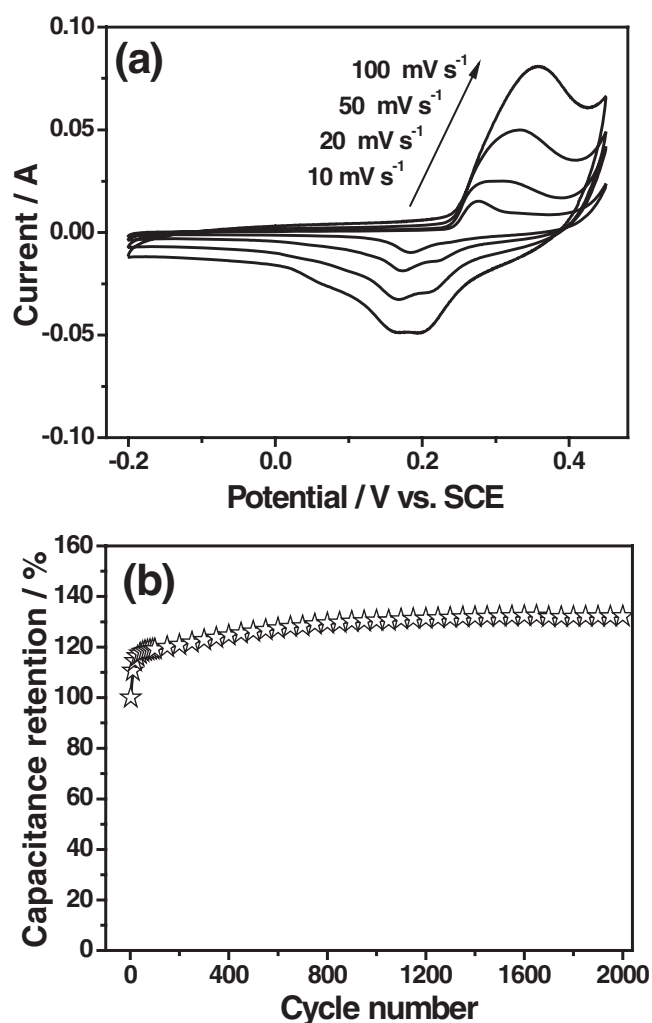


**Figure 3.** Electrochemical performances of CGS. a) CV results measured at scan rates of 10, 20, 50, and  $100 \text{ mV s}^{-1}$ . b) Variations of specific capacitance versus the cycle number measured at a scan rate of  $200 \text{ mV s}^{-1}$  in 6 M KOH within the potential range from  $-0.2$  to  $0.45$  V (versus saturated calomel electrode (SCE)).

to  $0.15$  V, suggesting that the capacitance attributed to pseudocapacitance from cobalt hydroxide is about two times higher than that of double layer capacitance from graphene.

Specific capacitance of CGS, CNT/graphene (physical mixing), graphene and cobalt oxide/graphene at various scan rates ( $10$ – $100 \text{ mV s}^{-1}$ ) is also shown for comparison (Figure S6, see the Supporting Information). The incorporation of CNT into graphene whatever by CVD or physical mixing can not only improve the surface area of graphene materials, but also act as “spacer” to supply diffusion path, facilitating rapid transport of the electrolyte ions within the electrode material, resulting in the improvement of electrochemical properties of CNT/graphene materials. Therefore, CGS exhibits the maximum capacitance of  $385 \text{ F g}^{-1}$  compared with other electrode materials, meaning that the unique structure endows rapid transport of the electrolyte ions or electron throughout the electrode matrix and comprehensive utilization of pseudo and double-layer capacitance. In addition, the self discharge curve for CGS shows two clearly distinguishable effects (Figure S7, see the Supporting Information). Though a relatively fast voltage drop was observed in the first hour, the following voltage drop became much slower, implying that the open surface area of CGS is favorable for the charge redistribution process.<sup>[39]</sup>

Electrochemical stability of CGS at a scan rate of  $200 \text{ mV s}^{-1}$  for 2000 cycles is shown in Figure 3b. A capacitance increase of ca. 20% of the initial capacitance after 2000 cycles has been observed, and that should be due to the increased effective interfacial area between cobalt hydroxide and electrolyte with the increase of reaction time, demonstrating excellent electrochemical stability of such electrode material, which is crucial for practical application.

The significant improvement of the electrochemical performance of CGS is mainly attributed to the unique sandwich structure of graphene and CNTs. Firstly, the wall of CNTs acts as a structural buffer for the large volume expansion of cobalt hydroxide particles during the redox reaction, and has good electrical contact with the particles upon cycling. Secondly, the introduction of CNTs can provide diffusion path on the surface of graphene, facilitating the electrolyte ions' diffusion and migration in the electrode during rapid charge/discharge processes. Finally, the interconnection of CNTs with graphene can form a conductive network for the transport of electrons, thus reducing the internal resistance of the electrode.

In summary, 3D CNT/graphene sandwich structures with CNT pillars grown in between the graphene layers had been prepared by CVD. The unique structure endows the high-rate transportation of electrolyte ions and electrons throughout the electrode matrix and comprehensive utilization of pseudo and double-layer capacitance, resulting in excellent electrochemical performances. The supercapacitor based on CGS exhibits a specific capacitance of  $385 \text{ F g}^{-1}$  at  $10 \text{ mV s}^{-1}$  in 6 M KOH solution. After 2000 cycles, a capacitance increase of ca. 20% of the initial capacitance is observed, indicating excellent electrochemical stability of the electrode. This new carbon material is also expected to be useful as electrode material in Li-ion secondary batteries, as media for hydrogen storage, as catalysts for fuel cells, and as component for other clean energy devices.

## Experimental Section

**Material Synthesis:** GO was synthesized from natural graphite (300  $\mu\text{m}$ , Qingdao Graphite Company) by a modified Hummers method.<sup>[40]</sup> As-synthesized GO was suspended in water to give a brown dispersion, which was subjected to dialysis to completely remove residual salts and acids. As purified GO (0.09 g) was then dispersed in water to create a dispersion (0.5 mg mL<sup>-1</sup>). Exfoliation of GO was achieved by ultrasonication of the dispersion using an ultrasonic bath (KQ-600KDE, 600 W). After that, Co(NO<sub>3</sub>)<sub>2</sub>·6H<sub>2</sub>O (0.2 g) and urea (0.4 g) were added into the above suspension. Subsequently, the resulting suspension was heated using a microwave oven (Haier, 2450 MHz, 700 W) for 15 min. After filtration and desiccation, the sample was placed in a horizontal quartz tubular reactor, and heated to 750 °C at 20 °C min<sup>-1</sup> in Ar (99.999%) atmosphere with a flow rate of 300 sccm. Subsequently, H<sub>2</sub> (99.999%) and carbon dioxide (99.95%) were introduced in turn at the same temperature with a flow rate of 100 and 70 sccm, respectively, and kept these conditions for 30 min. Finally the system was cooled down to room temperature in Ar atmosphere. To investigate the effect of catalyst concentration and carbon source on the morphologies of carbon, the same process was used except adjusting the corresponding parameters.

CNT/graphene hybrid material was synthesized by thermal reduction as follows: Specifically, the CNTs used in this work were prepared by the catalytic decomposition of propylene on Fe/Al<sub>2</sub>O<sub>3</sub> catalyst in a nano-agglomerated fluidized-bed reactor.<sup>[41]</sup> CNTs was purified and cut in a mixture of H<sub>2</sub>SO<sub>4</sub>/HNO<sub>3</sub> (3:1) at 140 °C for 1 h, and then filtrated and washed with de-ionized water. The obtained CNTs were ultrasonicated in GO suspension (mass ratio of CNT/GO is 1:10) for 1 h. After filtration and desiccation, the sample was placed in a horizontal quartz tubular reactor, and kept at 750 °C for 1 h in Ar (99.999%) atmosphere with a flow rate of 300 sccm. For comparison, pure graphene was also prepared according to the process described above without the addition of CNTs.

**Material Characterization:** The as-prepared samples were characterized by XRD (TTR-III), SEM (Camscan Mx2600FE), TEM (JEM 2010), atomic force microscope (AFM, Nanoscope IIIa), X-ray photoelectron spectroscopy (XPS, PHI-5700) and Raman spectroscopy (Perkin Elmer 400F). The BET surface areas of the samples were measured at 77 K using NOVA 2000 (Quantachrome, USA).

All electrochemical measurements were done in a three-electrode setup: A Ni foam coated with CGS served as the working electrode, a platinum gauze electrode and a saturated calomel electrode (SCE) or Hg/HgO electrode served as counter and reference electrodes respectively. The measurements were carried out on a CHI 660C electrochemical workstation in a 6 M KOH aqueous electrolyte at room temperature. The fabrication of working electrodes was carried out as follows. Briefly, 75 wt% of composite powder was mixed with 20 wt% of carbon black in an agate mortar until a homogeneous black powder was obtained. To this mixture, 5 wt% poly(tetrafluoroethylene) was added with a few drops of ethanol. Then the mixtures were pressed onto nickel foam current collectors (1 cm × 1 cm) to fabricate electrodes, and dried at 100 °C for 12 h. The specific capacitance of the electrode can be calculated according to the following equation:

$$C = \frac{1}{\omega v (V_c - V_a)} \int_{V_a}^{V_c} I(V) dV \quad (1)$$

where  $C$  is the specific capacitance (F g<sup>-1</sup>),  $\omega$  is the mass of electroactive materials in the electrodes (g),  $v$  is the potential scan rate (mV s<sup>-1</sup>),  $V_c$  and  $V_a$  are the integration limits of the voltammetric curve (V) and  $I(V)$  denotes the response current density (A cm<sup>-2</sup>).

## Supporting Information

Supporting Information is available from the Wiley Online Library or from the author.

## Acknowledgements

The authors acknowledge financial support from the National High-Tech Research and Development Plan of China (2008AA03A186), the Provincial Key Technologies R & D Program of Heilongjiang (GA07A401-3) and the Fundamental Research Foundation of Harbin Engineering University (Project HEUFT07094).

Received: March 22, 2010  
Published online: July 22, 2010

- [1] Z. Chen, Y. Qin, D. Weng, Q. Xiao, Y. Peng, X. Wang, H. Li, F. Wei, Y. Lu, *Adv. Funct. Mater.* **2009**, *19*, 3420.
- [2] X. Wang, L. J. Zhi, N. Tsao, Z. Tomovic, J. L. Li, K. Mullen, *Angew. Chem. Int. Ed.* **2008**, *47*, 2990.
- [3] J. Yan, T. Wei, B. Shao, Z. J. Fan, W. Z. Qian, M. L. Zhang, F. Wei, *Carbon* **2010**, *48*, 487.
- [4] D. A. Dikin, S. Stankovich, E. J. Zimney, R. D. Piner, G. H. B. Dommett, G. Evmenenko, S. T. Nguyen, R. S. Ruoff, *Nature* **2007**, *448*, 457.
- [5] S. Park, K. S. Lee, G. Bozoklu, W. Cai, S. T. Nguyen, R. S. Ruoff, *Acc Nano* **2008**, *2*, 572.
- [6] C. Chen, Q.-H. Yang, Y. Yang, W. Lv, Y. Wen, P.-X. Hou, M. Wang, H.-M. Cheng, *Adv. Mater.* **2009**, *21*, 3007.
- [7] S. Stankovich, D. A. Dikin, G. H. B. Dommett, K. M. Kohlhaas, E. J. Zimney, E. A. Stach, R. D. Piner, S. T. Nguyen, R. S. Ruoff, *Nature* **2006**, *442*, 282.
- [8] T. Ramanathan, A. A. Abdala, S. Stankovich, D. A. Dikin, M. Herrera-Alonso, R. D. Piner, D. H. Adamson, H. C. Schniepp, X. Chen, R. S. Ruoff, S. T. Nguyen, I. A. Aksay, R. K. Prud'homme, L. C. Brinson, *Nat. Nanotechnol.* **2008**, *3*, 327.
- [9] D. W. Wang, F. Li, J. P. Zhao, W. C. Ren, Z. G. Chen, J. Tan, Z. S. Wu, I. Gentle, G. Q. Lu, H. M. Cheng, *Acc Nano* **2009**, *3*, 1745.
- [10] P. Blake, P. D. Brimicombe, R. R. Nair, T. J. Booth, D. Jiang, F. Schedin, L. A. Ponomarenko, S. V. Morozov, H. F. Gleeson, E. W. Hill, A. K. Geim, K. S. Novoselov, *Nano Lett.* **2008**, *8*, 1704.
- [11] J. S. Bunch, A. M. Van Der Zande, S. S. Verbridge, I. W. Frank, D. M. Tanenbaum, J. M. Parpia, H. G. Craighead, P. L. McEuen, *Science* **2007**, *315*, 490.
- [12] S. Park, R. S. Ruoff, *Nat. Nanotechnol.* **2009**, *4*, 217.
- [13] X. Xie, L. Ju, X. Feng, Y. Sun, R. Zhou, K. Liu, S. Fan, Q. Li, K. Jiang, *Nano Lett.* **2009**, *9*, 2565.
- [14] K. S. Novoselov, A. K. Geim, S. V. Morozov, D. Jiang, Y. Zhang, S. V. Dubonos, I. V. Grigorieva, A. A. Firsov, *Science* **2004**, *306*, 666.
- [15] J. J. Wang, M. Y. Zhu, R. A. Outlaw, X. Zhao, D. M. Manos, B. C. Holloway, *Carbon* **2004**, *42*, 2867.
- [16] Q. Kuang, S. Y. Xie, Z. Y. Jiang, X. H. Zhang, Z. X. Xie, R. B. Huang, L. S. Zheng, *Carbon* **2004**, *42*, 1737.
- [17] Y. Zhou, Q. L. Bao, L. A. L. Tang, Y. L. Zhong, K. P. Loh, *Chem. Mater.* **2009**, *21*, 2950.
- [18] C. Berger, Z. M. Song, T. B. Li, X. B. Li, A. Y. Ogbazghi, R. Feng, Z. T. Dai, A. N. Marchenkov, E. H. Conrad, P. N. First, W. A. de Heer, *J. Phys. Chem. B* **2004**, *108*, 19912.
- [19] Z. P. Zhu, D. S. Su, G. Weinberg, R. Schlogl, *Nano Lett.* **2004**, *4*, 2255.
- [20] Y. Wang, Z. Q. Shi, Y. Huang, Y. F. Ma, C. Y. Wang, M. M. Chen, Y. S. Chen, *J. Phys. Chem. C* **2009**, *113*, 13103.
- [21] S. Stankovich, D. A. Dikin, R. D. Piner, K. A. Kohlhaas, A. Kleinhammes, Y. Jia, Y. Wu, S. T. Nguyen, R. S. Ruoff, *Carbon* **2007**, *45*, 1558.
- [22] X. B. Fan, W. C. Peng, Y. Li, X. Y. Li, S. L. Wang, G. L. Zhang, F. B. Zhang, *Adv. Mater.* **2008**, *20*, 4490.
- [23] Z. Fan, K. Wang, T. Wei, J. Yan, L. Song, B. Shao, *Carbon* **2010**, *48*, 1686.
- [24] X. S. Du, Z. Z. Yu, A. Dasari, J. Ma, M. S. Mo, Y. Z. Meng, Y. W. Mai, *Chem. Mater.* **2008**, *20*, 2066.

- [25] X. Wang, L. J. Zhi, K. Mullen, *Nano Lett.* **2008**, *8*, 323.
- [26] V. C. Tung, L. M. Chen, M. J. Allen, J. K. Wassei, K. Nelson, R. B. Kaner, Y. Yang, *Nano Lett.* **2009**, *9*, 1949.
- [27] S. Z. Zu, B. H. Han, *J. Phys. Chem. C* **2009**, *113*, 13651.
- [28] X. Y. Yang, X. Dou, A. Rouhanipour, L. J. Zhi, H. J. Rader, K. Mullen, *J. Am. Chem. Soc.* **2008**, *130*, 4216.
- [29] E. Yoo, J. Kim, E. Hosono, H. Zhou, T. Kudo, I. Honma, *Nano Lett.* **2008**, *8*, 2277.
- [30] Q. Zhang, M. Q. Zhao, Y. Liu, A. Y. Cao, W. Z. Qian, Y. F. Lu, F. Wei, *Adv. Mater.* **2009**, *21*, 2876.
- [31] Z. G. Zhao, L. J. Ci, H. M. Cheng, J. B. Bai, *Carbon* **2005**, *43*, 663.
- [32] S. R. Wang, Y. Zhang, N. Abidi, L. Cabrales, *Langmuir* **2009**, *25*, 11078.
- [33] A. Serquis, X. Z. Liao, J. Y. Huang, Q. X. Jia, D. E. Peterson, Y. T. Zhu, *Carbon* **2003**, *41*, 2635.
- [34] R. K. Rana, Y. Koltypin, A. Gedanken, *Chem. Phys. Lett.* **2001**, *344*, 256.
- [35] X. Z. Liao, A. Serquis, Q. X. Jia, D. E. Peterson, Y. T. Zhu, H. F. Xu, *Appl. Phys. Lett.* **2003**, *82*, 2694.
- [36] S. R. C. Vivekchand, C. S. Rout, K. S. Subrahmanyam, A. Govindaraj, C. N. R. Rao, *J. Chem. Sci.* **2008**, *120*, 9.
- [37] M. D. Stoller, S. J. Park, Y. W. Zhu, J. H. An, R. S. Ruoff, *Nano Lett.* **2008**, *8*, 3498.
- [38] A. B. Yuan, S. A. Cheng, J. Q. Zhang, C. N. Cao, *J. Power Sources* **1999**, *77*, 178.
- [39] B. E. Conway, *Electrochemical Supercapacitors: Scientific Fundamentals and Technological Applications*, Kluwer Academic/Plenum, New York, **1999**.
- [40] W. S. Hummers, R. E. Offeman, *J. Am. Chem. Soc.* **1958**, *80*, 1339.
- [41] Y. Wang, F. Wei, G. H. Luo, H. Yu, G. S. Gu, *Chem. Phys. Lett.* **2002**, *364*, 568.